Ab-initio calculations of the crystal field and phonon dispersions in $CePd_2Al_2$ and $LaPd_2Al_2$

D. Legut[1], M. Diviš[2], P. Doležal[2], P. Javorský[21,2]

[1]*IT4Innovations Center, VSB-Technical University of Ostrava, 17.listopadu 15, 708 33 Ostrava, Czech Republic*

[2]*Charles University, Faculty of Mathematics and Physics, Department of Condensed Matter Physics, Ke Karlovu 5, 121 16 Prague 2, Czech Republic*

Abstract

$CePd_2Al_2$ crystallizes in the $CaBe_2Ge_2$-type tetragonal structure ($P4/nmm$, 129) and undergoes a phase transition to the orthorhombic $Cmme$ structure at around 13 K. Its inelastic neutron spectra reveal an additional magnetic excitation that was ascribed to electron-phonon interaction leading to a formation of a new quantum quasi-bound vibron state. We present the first-principles calculations of the crystal field excitations and lattice dynamics calculations of the phonon dispersions to compare with the experimental data. The calculated crystal field energy splitting in $CePd_2Al_2$ agree well with the model used to describe the experimental neutron scattering spectra. The first excited crystal field level moves to higher energies when undergoing the transformation from tetragonal to orthorhombic structure, in agreement with experiment. The lattice dynamics calculations show that in both tetragonal and orthorhombic structures there are no imaginary modes for any q-wave vector within the Brillouin zone and therefore the lattice structures are stable. The phonon dispersions and density of states are calculated for both crystal structures of $CePd_2Al_2$ and its nonmagnetic counterpart $LaPd_2Al_2$. The results generally agree well with the experimental data including the high phonon density of states around 12 meV. The phonon density of states is also used to calculate the lattice heat capacity and compared with the experiment.

PACS numbers:

I. INTRODUCTION

The tetragonal CeT_2X_2 compounds (where R = rare earth, T = transition metal d-element and X = p-metal) form a large group of materials which exhibit various interesting physical properties as heavy-fermion behavior, valence-fluctuations, non-Fermi-liquid behavior or unconventional superconductivity.[1–5] These interesting properties stem from competition between RKKY and Kondo interactions and a strong influence of crystal field surrounding the Ce ions. The observation of an additional magnetic excitation in the neutron scattering spectra of $CePd_2Al_2$ is another interesting phenomenon.[6,7] The existence of three excitations from the ground state of Ce^{3+} ions cannot be explained in terms of pure crystal field splitting and was ascribed to electron-phonon interaction leading to a formation of a new quantum quasi-bound vibron state similar to $CeAl_2$[8,9] and $CeCuAl_3$[10]. This strong magneto-elastic coupling between orbital and lattice degrees of freedom and the resulting magneto-phonon mode have been described within the Thalmeier-Fulde model in the case of cubic $CeAl_2$.[11]

$CePd_2Al_2$ crystallizes in the $CaBe_2Ge_2$-type tetragonal structure ($P4/nmm$, 129) and undergoes a phase transition to the orthorhombic $Cmme$ structure at around $T_{\rm struc}^{\rm CePd_2Al_2} = 13$ K[6,12–14]. Similar structural phase transition is observed also in $LaPd_2Al_2$[6,12] excluding a magneto-elastic origin of the phase transition. The structural instability is not unusual in this family of compounds. Phase transition from tetragonal to a lower symmetry structures are observed e.g. in $CeNi_2Sn_2$,[15] $CePt_2Sn_2$,[15] $CeRh_2Sb_2$,[16] $CePt_2Ge_2$[17] or $CePd_2Ga_2$.[18,19] The magnetic properties of $CePd_2Al_2$ are characterized by an antiferromagnetic order below $T_{\rm N} = 2.7$ K[13]. The ground state magnetic structure is an amplitude modulated wave described by an incommensurate propagation vector $\vec{k} = (\delta_x, \frac{1}{2} + \delta_y, 0)$ with $\delta_x = 0.06$ and $\delta_y = 0.04$. The magnetic moments order antiferromagnetically within the planes stacked along the c-axis and are arranged along the direction close to the orthorhombic a-axis[7]. The recent neutron scattering experiment provided a clear link between the observed magnetic excitations and structural properties of $CePd_2Al_2$. The comparison of magnetic excitations measured above and below 13 K, where the structural transition from tetragonal to orthorhombic structure occurs, shows a strong shift of the energy of the first excited level to higher energies when cooling below 13 K.[7] The other two excitations are almost unaffected by this transition. These results motivated our ab-initio calculations of the phonon spectra and crystal field

excitations in both structural phases of $CePd_2Al_2$ to explore origin of the experimentally observed changes in energy spectra.

II. COMPUTATIONAL DETAILS

We performed first-principles electronic structure calculations using the general potential linearised augmented plane wave method (APW + lo, WIEN2k)[20]. The Kohn-Sham equations were solved within the generalized gradient approximation (GGA)[21]. The relativistic effects were treated using scalar relativistic approximation. Atomic sphere radii (AS) of 2.5, 2.1 and 1.8 Bohr radius (1 Bohr radius = 52.9177 pm) were chosen for Ce, Pd and Al, respectively. About 1400 linearized augmented plane waves (140 per atom) were used in the interstitial region and the highest value of 12 in the expansion of radial wave functions inside the AS to represent the valence states. The correlated Ce 4f states were treated in the open-core approximation and thus are characterized by integer number occupation $4f^1$. We have carefully checked that the calculation with these parameters converge. The first principles crystal field (CF) calculations were performed using the method described in Refs[22]. Within this method, the electronic structure and ground states charge density is obtained using the full potential APW + lo method. The CF parameters of the microscopic CF hamiltonian originate from the aspherical part of the total single particle DFT potential in the crystal. To eliminate the self interaction, the self-consistent procedure is first converge with the $4f$ electrons in core[22], which is the open-core approximation used in this work.

To obtain the dynamical properties the Hellmann-Feynman (HF) forces acting on the atoms starting from the equlibrium are required. For that we have utilized the unspin-polarized density functional theory method implementing the projector-augmented wave (PAW) formalism[23,24] to describe the electron-ion interactions. The approximation for the exchange-correlation potential was used the same as in WIEN2k calculations, i.e. GGA. The Kohn-Sham wave functions are expanded into plane waves up to a cutoff energy of 600 eV. The valence electrons of cerium, lanthanum, palladium, and aluminium atoms are represented by configurations of $5s^25p^65d^16s^2$, $5s^25p^64f^15d^16s^2$, $5s^14d^9$, and $3s^23p^1$, respectively. The calculations for the geometry optimazation used the $13 \times 13 \times 8(18 \times 18 \times 8)$ Monkhorst-Pack mesh of **k**-points for the orthorhombic(tetragonal) phase and the convergence criteria for the system's total energy and residual HF forces were of 10^{-7} eV and 10^{-4}

eV/Å, respectively.

The dynamical properties of the both $LaPd_2Al_2$ and $CePd_2Al_2$ lattice are obtained within the quasi-harmonic approximation and the direct method[25,26], which utilizes the DFT calculated HF forces acting on all atoms in a given supercell. Phonons are calculated for the supercells composed of 80 atoms (16 Ce(La), 32 Pd and 32 Al atoms), which are created from the optimized unit cells. Such supercells were found to be large enough to avoid contributions from atoms belonging to the periodic images, as confirmed by the elements of the force constant matrices which decay by more than three orders of magnitude at the distances smaller than the boundaries of the supercells. The Brillouin zone integration is performed with the reduced number of k-points $7 \times 7 \times 3(9 \times 9 \times 3)$ for the tetragonal (orthorhombic) phases. The non-vanishing HF forces required to construct respective dynamical matrix $\mathbf{D}(\mathbf{k})$ are generated by displacing the symmetry non-equivalent Ce(La), Pd and Al atoms from their equilibrium positions by the amplitude of ± 0.01 Å. Hence, for each configuration the total number of the calculated displacements amounts to 10 for both phases.

III. RESULTS AND DISCUSSION

The crystal field parameters and corresponding energy levels have been calculated assuming the two crystal structures of $CePd_2Al_2$ - high-temperature tetragonal ($CaBe_2Ge_2$-type) and low-temperature orthorhombic $Cmme$. The structural parameters have been taken from experiment.[7] The results are summarized in Table I both for tetragonal and orthorhombic Ce positions in the corresponding crystal structures. Both CF hamiltonians are dominated by second order term B20. This is the reason that the full splitting of the Ce^{3+} ground state multiplet remains similar for both tetragonal and orthorhombic phases. In the tetragonal structure, the second excited state lies at 11.8 meV what perfectly fits to energy of the hypothetical crystal field level assumed around 12 meV when analyzing the neutron scattering data[7]. The energy of this level changes only marginally when going from the tetragonal to the orhorhombic phase. The first excited level is calculated to be at 3.6 meV what is noticeably higher than the experimental value of 1.4 meV.[7] Possible explanation can be the complete neglect of hybridization in our first principles CF calculations. In compounds the hybridization of $4f$ states with valence states is very sensitive to the details of position of the $4f$ levels[27]. This crystal field level then considerably shifts to higher energies when

	B20	B22	B40	B42	B44	Δ_1	Δ_2
tetragonal	0.655	0.0	0.109×10^{-2}	0.0	0.173×10^{-1}	3.6	11.8
orthorhombic	0.628	-0.389	0.104×10^{-2}	-0.405×10^{-2}	-0.127×10^{-1}	4.8	12.2

TABLE I: The calculated crystal field parameters for tetragonal and orthorhombic phase of $CePd_2Al_2$ in Steven's notation Blm∗Olm. The meV units are used for both Blm and the energy splitting Δ.

$CePd_2Al_2$	a(Å)	b(Å)	c(Å)	z_{Ce}	z_{Pd}	z_{Al}
tetragonal	4.435(4.415)	-	10.090(9.874)	0.752	0.372	0.123
orthorhombic	6.274(6.268)	6.271(6.132)	10.089 (9.886)	0.753(0.756)	0.372 (0.371)	0.124(0.119)
$LaPd_2Al_2$	a(Å)	b(Å)	c(Å)	z_{La}	z_{Pd}	z_{Al}
tetragonal	4.451(4.441)	-	10.087(9.896)	0.753(0.749)	0.371(0.376)	0.121(0.138)
orthorhombic	6.334(6.313)	6.242(6.194)	10.105 (9.921)	0.752(0.745)	0.371(0.377)	0.129(0.149)

TABLE II: The calculated lattice paramters a, b, c in Å and internal degrees of freedom (z_X, X=Ce/La,Pd,Al). The experimental parameters in brackets for the Ce-phase and La-phase are taken from Ref.[7,19] and Ref.[19], respectively.

undergoing transition to the orthorhombic phase. This is in a qualitative agreement with the experimental observation[7].

Prior to the investigation of the lattice dynamics the geometrical optimizations need to be performed for the tetragonal $P4/nmm$ and orthorhombic $Cmme$ phases of $CePd_2Al_2$ and $LaPd_2Al_2$. Lattice parameters as well as the optimized internal degrees of freedom are summarized and compared to the experimental data in Table II. Calculated lattice constants agree well with the recorded ones, being slightly higher, but no more than 2%, than measured ones. This is a typical feature of the PBE functional for the exchange-correlations effects that tends to underestimate the binding energy. The overall agreement is therefore very good. Also the relaxed internal degrees of freedom, z-component of the Wyckoff positions (for details see Ref.[7]) show excellent agreement.

Lattice dynamics was investigated for both $CePd_2Al_2$ and $LaPd_2Al_2$. The dispersion relations of orthorhombic and tetragonal structures are shown in Figs. 1,2, respectively. In

both structures there are no imaginary modes for any q-wave vector within the Brillouin zone and therefore the lattice structures are stable. $CePd_2Al_2$ in both structures has higher slopes, see *e.g.* the ones between the Γ and Z point, *i.e* along the [00ζ] direction that indicates higher elastic stiffness along the *c*-axis. Another difference concerns the degeneracy of the transversal modes in the case of the tetragonal structure that is much higher in the case of $LaPd_2Al_2$ with respect to $CePd_2Al_2$, see transversal modes *e. g.* along Γ to X and Γ to M, respectively.

The total and partial phonon density of states (DOS), for definition see *e.g.* Ref.[28], for both $CePd_2Al_2$ and $LaPd_2Al_2$ are depicted in Figs. 3 and 4, respectively. The total phonon DOS for both compounds is very similar as regard frequency range owing to the fact that the mass difference is also small (M_{Ce}=140.115, M_{La}=138.906). Optical and acoustic frequencies are separated in both compounds and structures by a gap in frequency range between ca. 4.4-6.5 THz. The low frequency vibrations, in the range of 0-4.4 THz are dominated by the motions of the rare earth metal as well as palladium. The Al atoms vibrate at much higher frequencies. Here, the shape of the spectra for tetragonal structure is also very similar between both rare earths based compounds with higher frequencies of the $CePd_2Al_2$. In contrast the orthorhombic structure shows a large shift of phonon DOS at the higher frequencies (Al vibrations) for the Ce- vs. $LaPd_2Al_2$ compound. Please note the distinction of frequency range of vibrations for the Al atoms, *i.e.* a clear difference between motions of atoms with Wyckoff positions 2*c* and 2*b* and 4*b* and 4*g* of tetragonal and orhorhombic structure, respectively. Also, for the orthorhombic structure the center of mass of the lower frequency of phonon DOS (R+Pd atoms) is shifted by ca 0.5 THz to higher frequencies for the $CePd_2Al_2$ with respect to the $LaPd_2Al_2$. There is also a remarkable shift of the low frequency DOS (R+Pd atoms) to higher energies in the orthorhombic structure of $CePd_2Al_2$ with respect to the tetragonal one. No such shift occurs for $LaPd_2Al_2$.

The total phonon density of states could be used to estimate the Debye temperature (Θ_D). Using lower frequencies 0-2THz and fitting function of $\Theta_D(\omega) = a\omega^2$, where a is a parameter for the fitting function of$\Theta_D = (\frac{9N}{a})^{1/3}$, where N is number of atoms in unit cell. The total DOS of $LaPd_2Al_2$ in both structures is similar, see Figs. 3 and 4, the estimated Debye temperatures are practically the same, $\Theta_D = 185(183)K$ for the orhorhombic(tetragonal) structure, respectively. Slighlty larger difference is in the case of $CePd_2Al_2$, here $\Theta_D = 189K$ vs. $205K$ between the tetragonal and orthorhombic one. Calculated Debye temperature for

$LaPd_2Al_2$ is considerably larger than the one obtained from measurements of specific heat and electric resistivity, ($\Theta_D = 117 - 127$ K[29], however in a very good agreement with the value obtained by Kitagawa et al., $\Theta_D = 174$ K[18]. In fact, results of the models used in both references are in agreement considering that the former one considers only the three acoustic branches for the Θ_D evaluation at very low temperatures while Θ_D in the latter one corresponds to the total number of 15 phonon branches.Our calculation is in line with the latter approach.

The calculated phonon DOS enable us to evaluate some thermodynamical quantities that are phonon-dependent. Here, we restrict our investigations to phonons calculated within the harmonic approximation (quasi-harmonic approximations) and analyze mean-squared amplitudes of atomic vibrations (U_{ij}) ands the lattice contribution to the heat capacity as a function of temperature. Mean-squared vibrational amplitudes of a given atom in crystal lattice constitute a second-rank symmetric tensor and they can be expressed by the diagonal and off-diagonal partial phonon DOS[28,30]. In Fig. **??** the MSD in $\mathring{A}^2$ is displayed for the $LaPd_2Al_2$..

The calculated lattice heat capacity at constant pressure (C_p) is compared with the measured data in Fig. 6 for $LaPd_2Al_2$. The specific heat of $LaPd_2Al_2$ is reproduced with a very good agreement including the low-temperature part (just above the T_c). The direct comparison for $CePd_2Al_2$ is not possible because the specific heat of the Ce material includes also significant magnetic contribution and a large heat capacity connected with the structural phase transition at 13 K. Neverthelless, the calculated heat capacity at constant pressure shows the negligible influence of the electronic contribution, to be linearly dependent along the temperature and corresponding to the number of electronic states at Fermi level (Sommerfeld coefficient). This become more significat over T¿XXXK, whereas at all determined temperatures the lattice contributions are dominating as expected, see Fig. XXX.

Let us finally relate all the calculated results to the inelastic neutron scattering data[7] what was a primary goal of this work. The simultaneous occurrence of the high density of phonon states and the CF level at the same energy as the key preriquisite for the magnetoelastic coupling and formation of the vibron states. Our present calculations are fully in agreement with such a scheme. The high phonon density of states around 12 meV is i) well in agreement with the experimental observation[7] and ii) appears at energy which is the same or very close to the calculated energy of the second CF excited state. We note that there is no

CF excitation experimentally observed around 12 meV, but it is just the energy of the hypothetical CF level assumed when analyzing the neutron scattering data[7].

When undergoing the structural transition from tetragonal to orthorhombic structure at 13 K, the experiment revealed a strong shift of the first magnetic excitation to higher energies[7]. Such a shift is qualitatively well reproduced by our first-principles electronic structure calculations although there is a certain quantitative difference between the experimental and calculated energy as discussed above. The experimentally observed development of the energy of the first excited CF level can be thus primarily ascribed to CF changes when transforming from tetragonal to orthorhombic structure.

Our calculations show also some clear changes of the phonon spectra when comparing the tetragonal and orthorhombic case. As concern the low-energy part of the of $CePd_2Al_2$ phonon spectra, there is a clear shift of the DOS (R+Pd atoms) to higher energies in the orthorhombic structure with respect to the tetragonal structure. No such shift occurs for $LaPd_2Al_2$. This can point either to a different characteristics of the structural transition in $CePd_2Al_2$ and $LaPd_2Al_2$ (see also[19]).

The calculated lattice heat capacity at constant pressure (C_p) is compared with the measured data in Fig. 6 for $LaPd_2Al_2$. The specific heat of $LaPd_2Al_2$ is reproduced with a reasonably good agreement. Rather surprisingly, the calculation corresponding to the tetragonal lattice agrees almost perfectly with the experimental data while the data for the orthorhombic structure slightly exceed the measured values in the low-temperature part (just above the T_c). We remind that $LaPd_2Al_2$ undergoes the structural transition to the orthorhombic phase around 90 K[6,12,19], so we would expect better agreement with the orthorhombic lattice calculation at low temperatures. The direct comparison for $CePd_2Al_2$ is not possible because the specific heat of the Ce material includes also significant magnetic contribution and a large heat capacity connected with the structural phase transition at 13 K.

MSD, Cp, enegy difference with phonons and force constant, irreps

IV. CONCLUSIONS

The first-principles electronic structure calculations for $CePd_2Al_2$ lead to crystal field excitations at 3.6 meV and 11.8 meV for the tetragonal structure and at 4.8 meV and

12.2 meV for the orthorhombic structure. The change for the first excited level agrees qualitatively well with the experiment. The energy of the second excited level fits perfectly with the model used to describe the inelastic neutron scattering data.

The lattice dynamics calculations show that in both tetragonal and orthorhombic structures there are no imaginary modes for any q-wave vector within the Brillouin zone and therefore the lattice structures are stable. There is a large phonon DOS at around 12 meV in agreement with the experimental observation. The calculation indicate a shift of the low frequency DOS (R+Pd atoms) to higher energies in the orthorhombic structure of $CePd_2Al_2$ with respect to the tetragonal structure. No such shift occurs for $LaPd_2Al_2$.

V. ACKNOWLEDGEMENT

This work was supported by the Czech Science Foundation under Grant No. 17-04925J. D. L. acknowledges support by the European Regional Development Fund in the IT4Innovations national supercomputing center - path to exascale project, project number CZ.02.1.01/0.0/0.0/16_013/0001791 within the Operational Programme Research, Development and Education, by the grant No. 17-27790S of the Czech Science Foundations and Mobility grant No. 8J18DE004

[1] F. Steglich, J. Aarts, C.D. Bredl, W. Lieke, D. Meschede, W. Franz, H. Schäfer, Phys. Rev. Lett. 43 (1979) 1892.

[2] B. Bellarbi, A. Benoit, D. Jaccard, J.M. Mignot, H.F. Braun, Phys. Rev. B 30 (1984) 1182.

[3] T. Endstra, G.J. Nieuwenhuys, J.A. Mydosh, Phys. Rev. B 48 (1993) 9595.

[4] R. Movshovich, T. Graf, D. Mandrus, J.D. Thompson, J.L. Smith, Z. Fisk, Phys. Rev. B 53 (1996) 8241.

[5] D. Jaccard, K. Behnia, J. Sierro, Phys. Lett. A 163 (1992) 475.

[6] L.C. Chapon, E.A. Goremychkin, R. Osborn, B.D. Rainford, S. Short, Physica B 378-380 (2006) 819.

[7] M. Klicpera, M. Boehm, P. Doležal, H. Mutka, M. Koza, S. Rols, D. T. Adroja, I. Puente-Orench, J. Rodriguez-Carvajal, P. Javorský, Phys. Rev. B 95 (2017) 085107.

[8] M. Loewenhaupt, B.D. Rainford, F. Steglich, Phys. Rev. Lett. 42 (1979) 1709-1712.

[9] M. Loewenhaupt, W. Reichardt, R. Pynn, E. Lindley, J. Magn. Magn. Mater. 63-64 (1987) 73-75.

[10] D. T. Adroja, A. del Moral, C. de la Fuente, A. Fraile, E. A. Goremychkin, J.W. Taylor, A. D. Hillier, F. Fernandez-Alonso, Phys. Rev. Lett. 108 (2012) 216402.

[11] P. Thalmeier, P. Fulde, Phys. Rev. Lett. 49 (1982) 1588.

[12] M. Klicpera, P. Javorský, A. Hoser, J. Alloys Comp. 596 (2014) 167-172.

[13] M. Klicpera, P. Doležal, J. Prokleška, J. Prchal, P. Javorský, J. Alloys Comp. 639 (2015) 51-59.

[14] A. Tursina, E. Khamitcaeva, A. Gribanov, D. Gnida, D. Kaczorowski, Inorg. Chem. 54 (2015) 3439-3445.

[15] W.P. Beyermann, M.F. Hundley, p.C. Canfield, C. Godart, M. Selsane, Z. Fisk, J.L Smith, J.D. Thompson, Physica B 171 (1991) 373.

[16] T. Takabatake, T. Tanaka, Y. Bando, H. Fujii, N. Takeda, M. Ishikawa, I. Oguro, Physica B 230-232 (1997) 223-225.

[17] A. Dommann, F. Hullier, H.R. Ott, V. Gramlich, J. Less.-Common. Met. 110 (1985) 331.

[18] J. Kitagawa, M. Ishikawa, J. Phys. Soc. Japan 68 (1999) 2380-2383.

[19] P. Doležal, M. Klicpera, J. Prchal, P. Javorský, will be published.

[20] K. Schwarz, P. Blaha, G. Madsen, Comput. Phys. Commun. 147 (2002) 71.

[21] J.P. Perdew, K. Burke, M. Ernzerhof, Phys. Rev. Lett. 77 (1996) 3865.

[22] M. Diviš, J. Rusz, H. Michor, G. Hilscher, P. Blaha, K. Schwarz, J. Alloy Compd. 403 (2005) 29.

[23] G. Kresse and J. Furthmüuller, Phys. Rev. B **54**, 11169 (1996).

[24] G. Kresse and J. Furthmüuller, Comput. Mater. Sci. **6**, 15 (1996).

[25] K. Parlinski, Z. Q. Li, and Y. Kawazoe, Phys. Rev. Lett. **78**, 4063 (1997).

[26] A. Togo, L. Chaput, I. Tanaka, G. Hug, Phys. Rev. B, **81**, 174301 (2010).

[27] P. Novak, M. Diviš, phys. stat. sol. (b) 244 (2007) 3168.

[28] U. D. Wdowik and D. Legut, J. Phys. Cond. Mat. **21**, 275402 (2009).

[29] M. Klicpera, J. Pásztorová, P. Javorský, Superconduc. Science Techn., 27 (2014) 085001.

[30] U. D. Wdowik and K. Parlinski, Phys. Rev. B **75**, 104306 (2007).

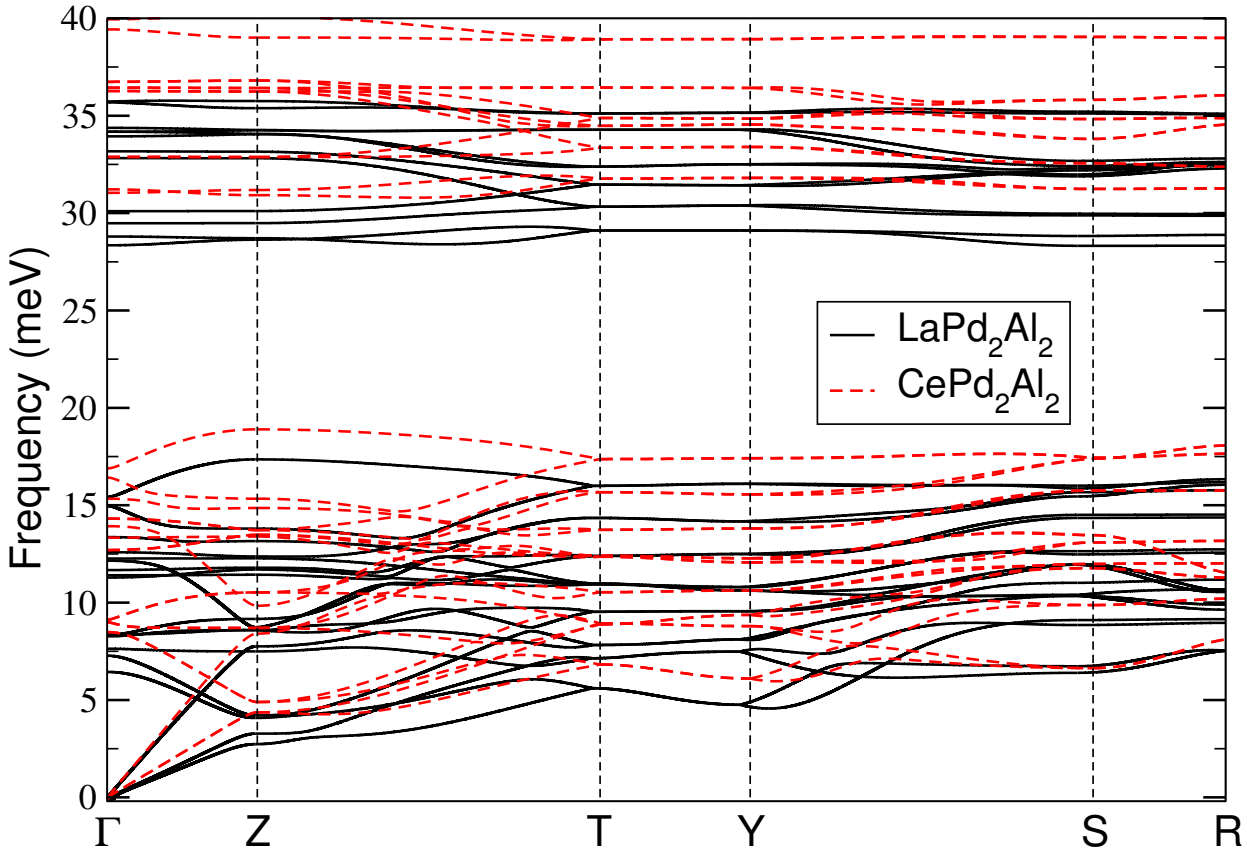

FIG. 1: Phonon dispersion relation of $LaPd_2Al_2$ and $CePd_2Al_2$ in ortorhombic structure $(Cmme, 67)$.

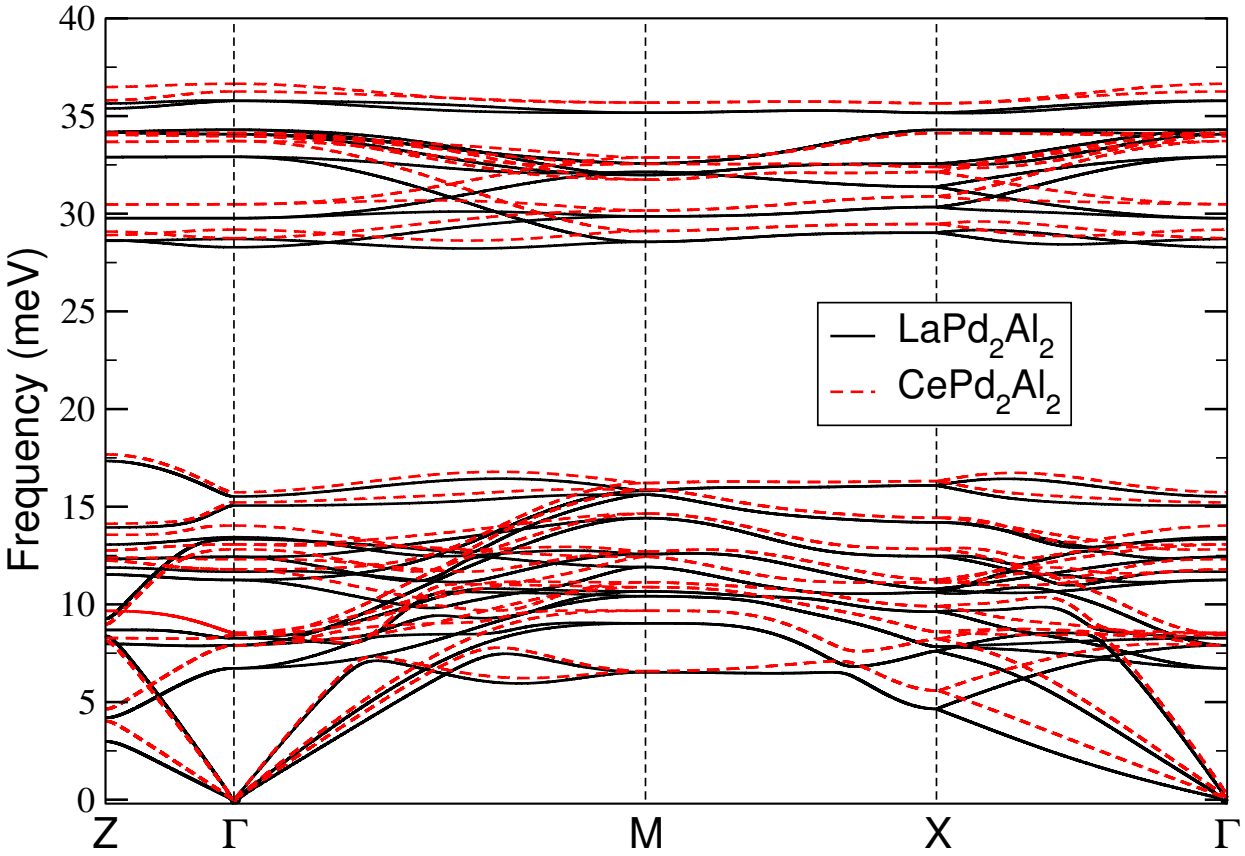

FIG. 2: Phonon dispersion relation of $LaPd_2Al_2$ and $CePd_2Al_2$ in tetragonal structure ($P4/mmm, 129$).

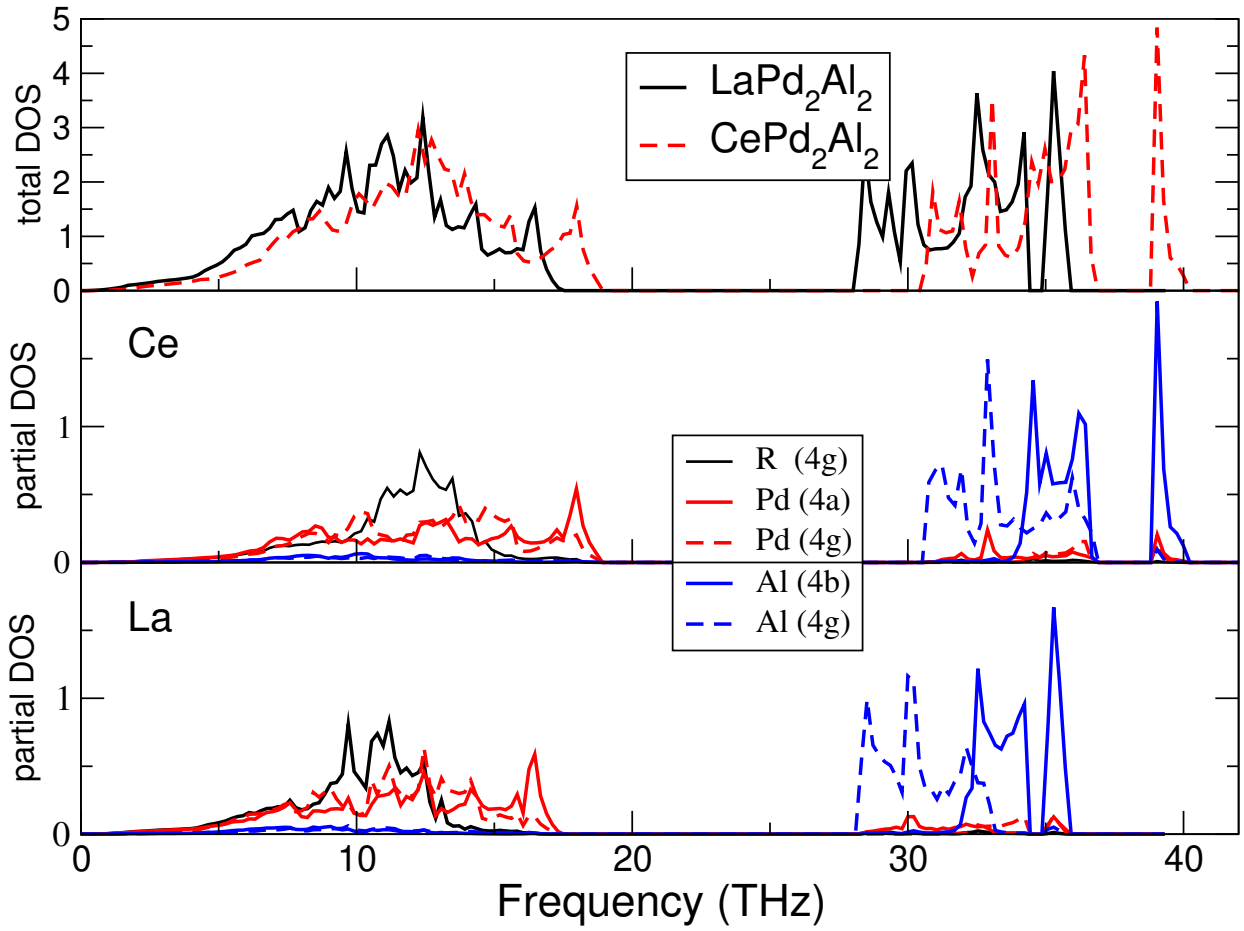

FIG. 3: Total and partial density of states in (states/THz) of $LaPd_2Al_2$ and $CePd_2Al_2$ in ortorhombic structure ($Cmme, 67$).

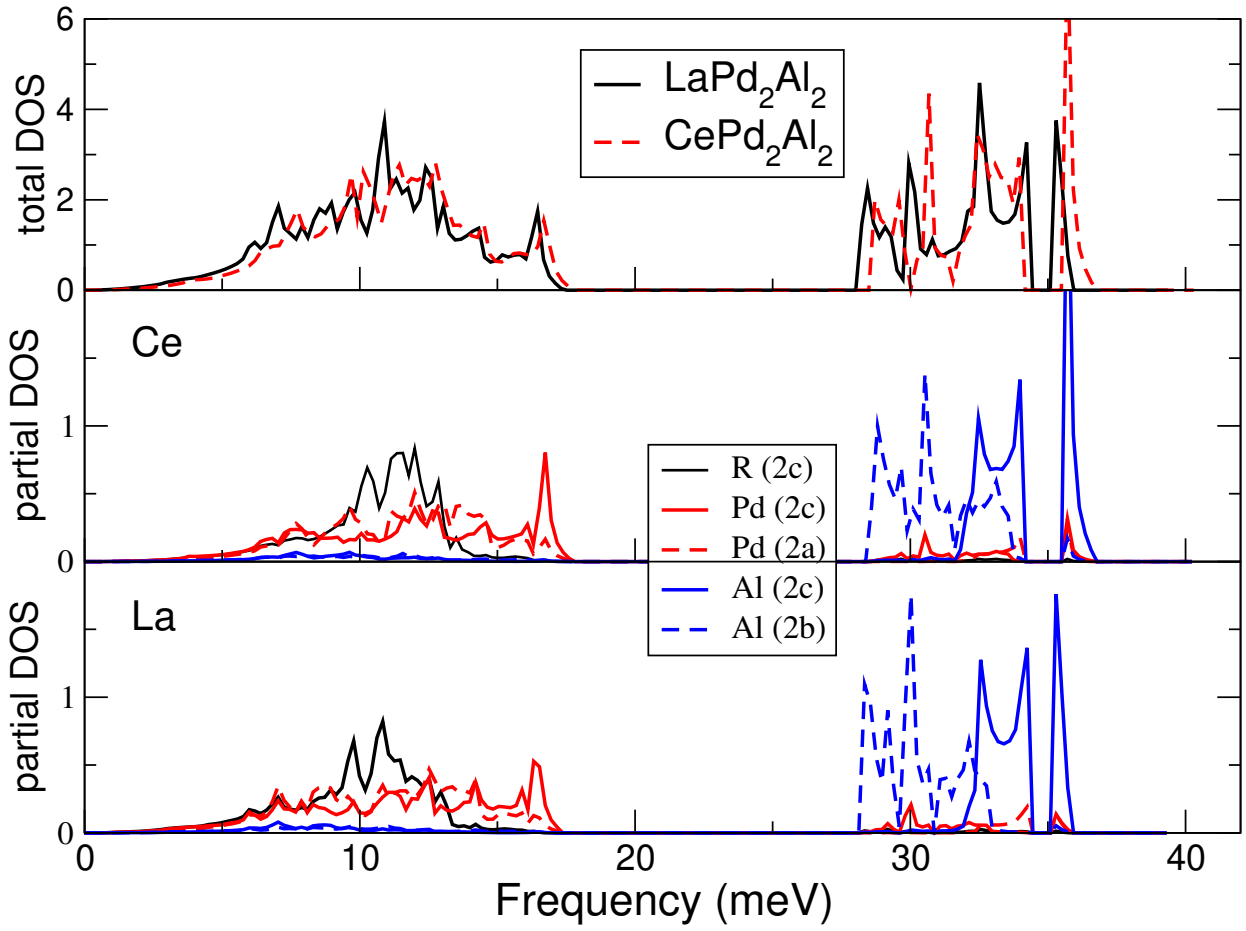

FIG. 4: Total and partial density of states in (states/THz) of $LaPd_2Al_2$ and $CePd_2Al_2$ in tetragonal structure ($P4/mmm, 129$).

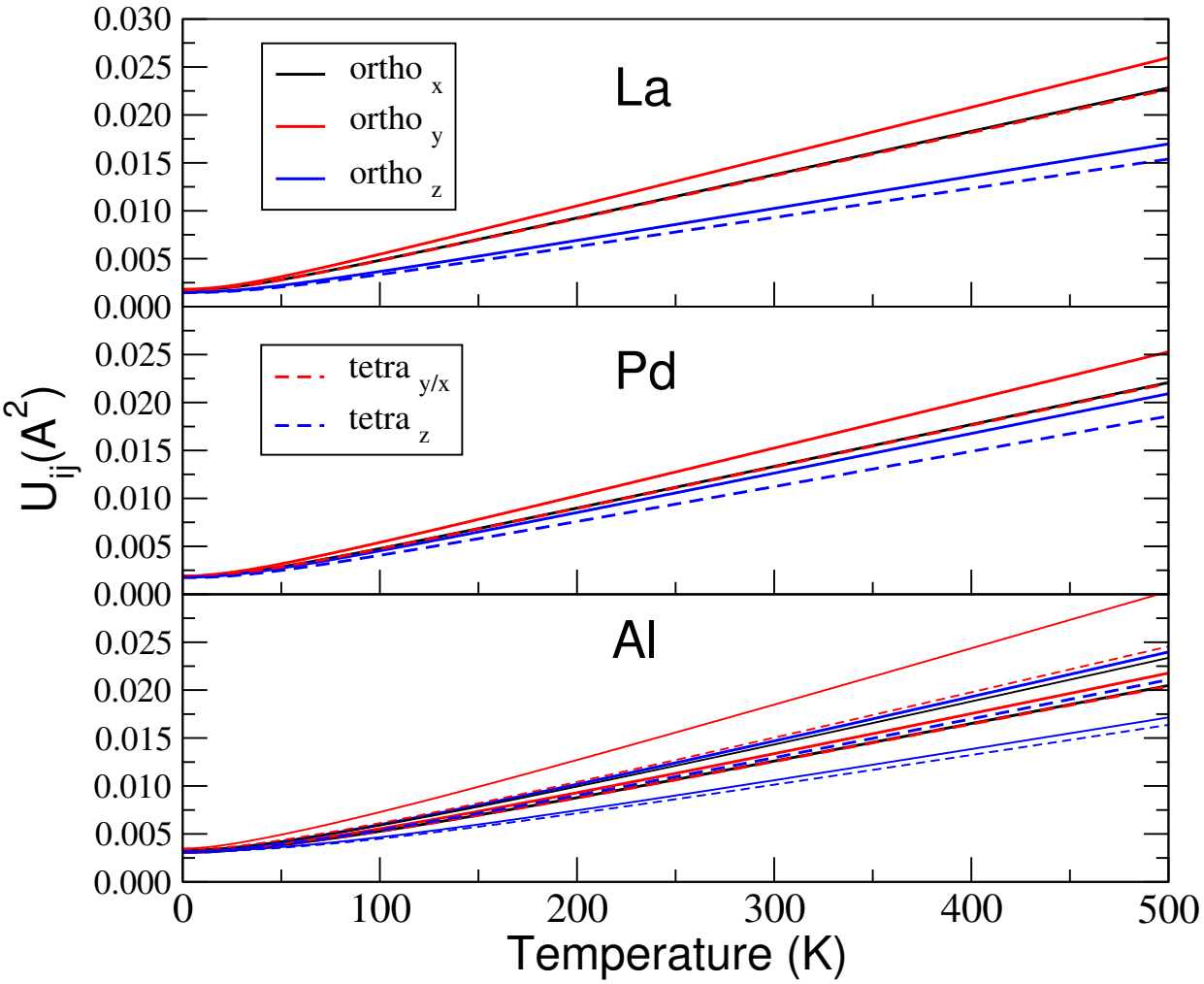

FIG. 5: Mean square displacement of the $LaPd_2Al_2$. The solid and dashed line mark for the orthorhombic and tetragonal structure, respetively.

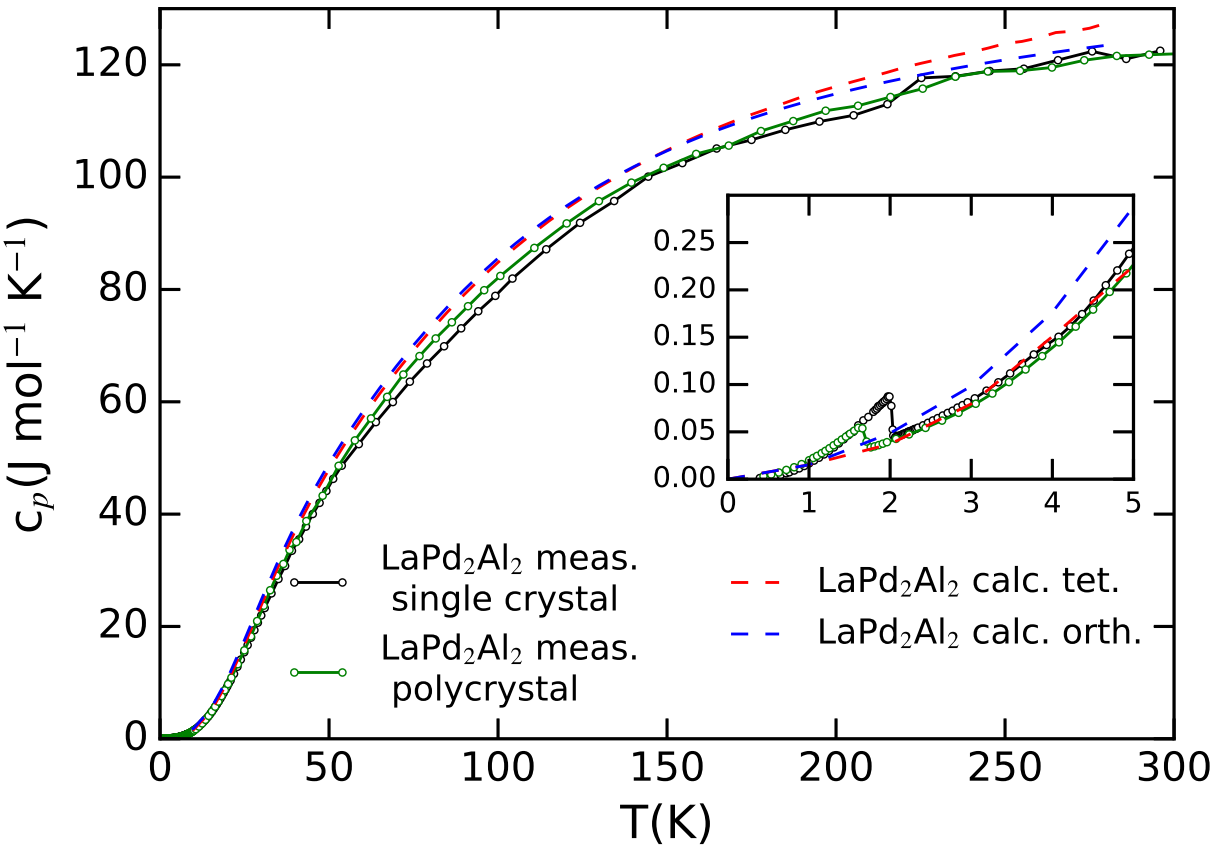

FIG. 6: Comparison of measured and calculated specific heat of $LaPd_2Al_2$. The calculated curve includes, beside the dominant phonon contribution, also the electronic part taking the experimentally determined gamma coefficient of 15mJmol−1K−2[29].